The Influence of Temperature on Ozone Production under varying NO_x Conditions – a modelling study

J. Coates[1], K. Mar[1] and T. Butler[1]

[1]Institute for Advanced Sustainability Studies, Potsdam, Germany

March 4, 2016

Abstract

Ground-level ozone is a secondary air pollutant produced during the degradation of emitted volatile organic compounds (VOCs) and nitrogen oxides (NO_x) in the presence of sunlight. As ozone production is dependent on photochemical processes, meteorological factors such as temperature influence ozone production. Temperature directly influences ozone production through speeding up the rates of the chemical processes producing ozone and increasing the emissions of VOCs, such as isoprene, from vegetation. In this study, we used a box model to reproduce the non-linear relationship of ozone on NO_x and temperature from previous observational studes. Faster chemistry was responsible for an increase in ozone of up to 20 ppbv while increased isoprene emissions added a further 11 ppbv of ozone under high-NO_x conditions. The shorter lifetime of peroxy nitrates with increased temperature was the main contributor to the increased production of ozone with temperature. At 40 °C, the thermal decomposition of peroxy nitrates was responsible for up to 45 % of the normalised O_x production. The rate of increase in ozone with temperature from our box model simulations was about half rate of the increase in ozone with temperature over central Europe compared to both observed and WRF-Chem simulations. The missing sensitivity in our simulations compared to observations and 3D model output is related to the indirect influence of temperature on ozone production not included in our experiment.

1 Introduction

Surface-level ozone (O_3) is a secondary air pollutant formed during the photochemical degradation of volatile organic compounds (VOCs) in the presence of nitrogen oxides ($NO_x \equiv NO + NO_2$). Due

1

to the photochemical nature of ozone production, meteorological variables such as temperature strongly influence ozone production (Jacob and Winner, 2009). Otero et al. (2016) showed that temperature was a major meteorological driver for summertime ozone in many areas of central Europe.

Temperature primarily influences ozone production in two ways: speeding up the reaction rates of many chemical reactions leading to ozone production, and increasing emissions of VOCs from biogenic sources (BVOCs). While emissions of anthropogenic VOCs (AVOCs) are generally not dependent on temperature, evaporative emissions of AVOCs increase with temperature (Rubin et al., 2006). The review of Pusede et al. (2015) provides further details of the temperature-dependent processes impacting ozone production.

Studies over the US (Sillman and Samson, 1995; Dawson et al., 2007; Pusede et al., 2014) noted that increased temperatures tend to lead to higher ozone levels, often exceeding local air quality guidelines. Some studies (Sillman and Samson, 1995; Dawson et al., 2007) included regional modelling to simulate the observed increases in ozone with temperature. In these studies, the increase of ozone with temperature was attributed to the shorter lifetime of PAN (peroxy acetyl nitrate) at higher temperatures and increased emissions of BVOCs, in particular isoprene, from vegetation.

Pusede et al. (2014) used an analytical model constrained by observations over San Joaquin Valley, California to infer a non-linear relationship of ozone production with temperature and NO_x, similar to the well-known non-linear relationship of ozone production on NO_x and VOC levels (Sillman, 1999). Morever, Pusede et al. (2014) showed that temperature can be used as a surrogate for VOC levels when considering the relationship of ozone across NO_x gradients.

Environmental chamber studies have also been used to analyse the relationship of ozone with temperature. The chamber experiments of Carter et al. (1979) and Hatakeyama et al. (1991) showed increases in ozone from a VOC mix with temperature linked to increased PAN decomposition at temperatures greater than 303 K.

Despite many studies considering the effects of temperature on ozone production from an observational and chamber study perspective, there are no modelling studies (to our knowledge) focusing on the detailed chemical processes of the influence of temperature on ozone production under different NO_x conditions. Regional modelling studies (using a single chemical mechanism) have concentrated on reproducing ozone levels over regions with known meteorology and NO_x conditions then only varying the temperature. These modelling studies did not consider the

relationship of ozone with NO_x with temperature. The review of Pusede et al. (2015) also highlights a lack of modelling studies looking at the non-linear relationship of ozone on temperature under different NO_x conditions.

Comparisons of different chemical mechanisms, such as Emmerson and Evans (2009) and Coates and Butler (2015), showed that different representations of tropospheric chemistry influenced ozone production. These studies did not consider whether the ozone-temperature relationship differed between chemical mechanisms. The study of Rasmussen et al. (2013) also noted that changing the chemical mechanism used by a model may also change the simulated ozone-temperature relationship. Comparing the ozone-temperature relationship predicted by different chemical mechanisms is important for simulating air quality in the future with an expected increase in heatwaves.

In this study, we use an idealised box model to determine how ozone levels vary with temperature under different NO_x conditions. We determine whether faster chemical reaction rates or increased BVOC emissions have a greater influence on instantaneous ozone production with higher temperature under different NO_x conditions. Furthermore, we compare the ozone-temperature relationship produced by different chemical mechanisms by repeating all simulations with various chemical mechanisms.

2 Methodology

2.1 Model Setup

We used the MECCA box model to determine the important gas-phase chemical processes for ozone production under different temperatures and NO_x conditions. The MECCA box model was set up as described in Coates and Butler (2015) and updated to include vertical mixing with the free troposphere using a diurnal cycle for the PBL height. The supplementary material includes further details of these updates.

Simulations were performed to broadly simulate urban conditions representative of central Europe with equinoctical conditions. The simulations started at 06:00 with a total run time of two days. Methane was fixed at 1.7 ppmv throughout the model run, carbon monoxide (CO) and ozone were initialised at 200 ppbv and 40 ppbv and then allowed to evolve freely throughout the simulation. All VOC emissions were held constant until noon of first day simulating a plume of freshly-emitted VOC.

Separate box model simulations were performed by systematically varying the temperature between 288 and 313 K (15 – 40 °C). The only source of NO_x emissions in the box model was a constant source of NO emissions. Box model runs were performed with the NO emissions systematically varied between 5.0×10^9 and 1.5×10^{12} molecules (NO) cm^{-2} s^{-1} at each temperature used in this study. At 20 °C, these NO emissions corresponded to peak NO_x mixing ratios of 0.02 ppbv and 10 ppbv respectively, this range of NO_x mixing ratios covers the NO_x conditions in pristine and urban conditions (von Schneidemesser et al., 2015).

All simulations were repeated using different chemical mechanisms to investigate whether the relationship of ozone with temperature across NO_x gradients changes using different representations of ozone production chemistry. The reference chemical mechanism was the near-explicit Master Chemical Mechanism, MCMv3.2, (Jenkin et al., 1997, 2003; Saunders et al., 2003; Rickard et al., 2015). The reduced chemical mechanisms in our study were Common Representative Intermediates, CRIv2 (Jenkin et al., 2008), Model for ozone and related chemical tracers, MOZART-4 (Emmons et al., 2010), Regional Acid Deposition Model, RADM2 (Stockwell et al., 1990) and the Carbon Bond Mechanism, CB05 (Yarwood et al., 2005). Coates and Butler (2015) described these chemical mechanisms and the implementation of these chemical mechanisms in MECCA. These reduced chemical mechanisms were chosen as they are commonly used by modelling groups in 3D regional and global models (Baklanov et al., 2014).

Model runs were repeated using a temperature-dependent and temperature-independent source of BVOC emissions to determine whether increased emissions of BVOC or faster chemistry is more important for the increase of ozone with temperature. MEGAN2.1 (Guenther et al., 2012) specified the temperature-dependent BVOC emissions of isoprene, Sect. 2.3 provides further details. As isoprene emissions are the most important on the global scale, we considered only isoprene emissions from vegetation (Guenther et al., 2006). Only isoprene emissions were dependent on temperature, all other emissions were constant in all simulations. In reality, many other BVOC are emitted from varying vegetation types (Guenther et al., 2006) and increased temperature can also increase AVOC emissions through increased evaporation (Rubin et al., 2006).

2.2 VOC Emissions

Emissions of urban AVOC over central Europe were taken from TNO-MACC_III emission inventory for the Benelux (Belgium, Netherlands and Luxembourg) region for the year 2011. TNO-MACC_III is the updated TNO-MACC_II emission inventory created using the same

Table 1: Total AVOC emissions in 2011 in tonnes from each anthropogenic source category assigned from TNO-MACC_III emission inventory and temperature-independent BVOC emissions in tonnes from Benelux region assigned from EMEP. The allocation of these emissions to MCMv3.2, CRIv2, CB05, MOZART-4 and RADM2 species are found in the supplementary material.

	Public Power	Residential Combustion	Industry	Fossil Fuel
Belgium	4494	9034	22152	5448
Netherlands	9140	12173	29177	8723
Luxembourg	121	44	208	1371
Total	13755	21251	62648	15542
	Solvent Use	Road Transport: Gasoline	Road Transport: Diesel	Road Transport: Others
Belgium	42809	6592	2446	144
Netherlands	53535	16589	3230	1283
Luxembourg	4482	1740	1051	6
Total	100826	24921	6727	1433
	Road Transport: Evaporation	Non-road Transport	Waste	BVOC
Belgium	210	6448	821	7042
Netherlands	1793	10067	521	1462
Luxembourg	324	643	0	2198
Total	2327	17158	1342	10702

methodology as Kuenen et al. (2014) and based upon improvements to the existing emission inventory during AQMEII-2 (Pouliot et al., 2015).

Temperature-independent emissions of isoprene and monoterpenes from biogenic sources were calculated as a fraction of the total AVOC emissions from each country in the Benelux region. This data was obtained from the supplementary data available from the EMEP (European Monitoring and Evaluation Programme) model (Simpson et al., 2012). Temperature-dependent emissions of isoprene are detailed in Sect. 2.3.

AVOC emissions were allocated to source categories defined by the different SNAP (Selected Nomenclature for Air Pollution) categories. Table 1 shows the quantity of VOC emissions from each source category and the temperature-independent BVOC emissions. These categorised AVOC emissions were assigned to chemical species and groups based on the country specific profiles for Belgium, the Netherlands and Luxembourg provided by TNO. Most individual chemical species are represented by the MCMv3.2, otherwise the individual contributions of a group of VOC were further split into individual components using the detailed speciation of Passant (2002). For example, 'xylenes' are one of the component chemical groups in many source

Figure 1: The estimated isoprene emissions (molecules isoprene cm^{-2} s^{-1}) using MEGAN2.1 at each temperature used in the study.
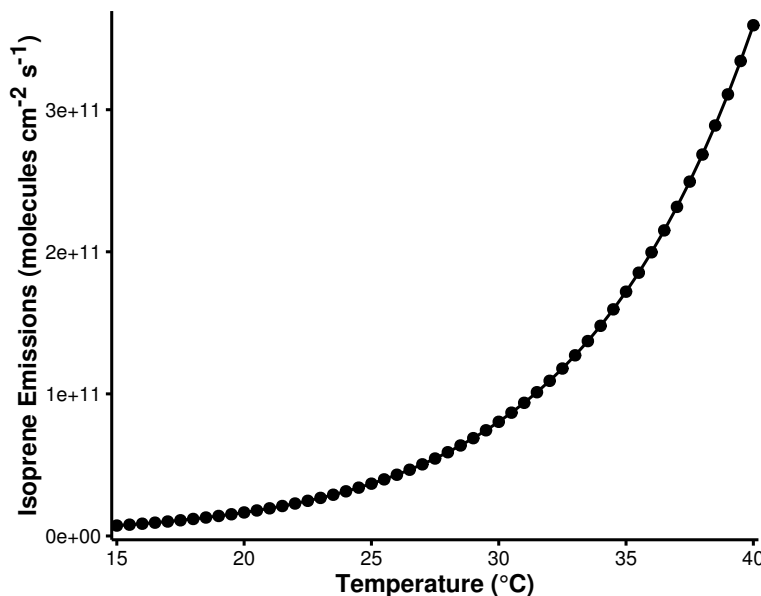
categories but the MCMv3.2 treats xylenes as the individual isomers (m-, o-, p-xylene) and the contributions of the individual isomers to a source category was provided by Passant (2002). This approach was also used in von Schneidemesser et al. (2016) to allocate AVOC emissions from different solvent sector speciations to MCMv3.2 species.

For simulations done with other chemical mechanisms, the VOC emissions represented by the MCMv3.2 were mapped to the mechanism species representing VOC emissions in each reduced chemical mechanism based on the recommendations of the source literature and Carter (2015). The VOC emissions in the reduced chemical mechanisms were weighted by the carbon numbers of the MCMv3.2 species and the emitted mechanism species, thus keeping the amount of emitted carbon constant between simulations. The supplementary data outlines the primary VOC and calculated emissions with each chemical mechanism.

2.3 Temperature Dependent Isoprene Emissions

Temperature-dependent emissions of isoprene were estimated using the MEGAN2.1 algorithm for calculating the emissions of VOC from vegetation (Guenther et al., 2012). Emissions from nature are dependent on variables including temperature, radiation and age but for the purpose of our study all variables except temperature were held constant.

The MEGAN2.1 parameters were chosen to give similar isoprene mixing ratios at 20 °C to the temperature-independent emissions of isoprene in order to compare the effects of increased

Table 2: Increase in ozone mixing ratio (ppbv) due to chemistry and emissions at 40 °C from reference temperature (20 °C) in the NO_x-regimes of Fig. 3.

Chemical Mechanism	Source of Difference	Increase in Ozone at 40 °C from 20 °C (ppbv)		
		Low-NO_x	Maximal-O_3	High-NO_x
MCMv3.2	Emissions	4.6	7.7	10.6
	Chemistry	6.8	12.5	15.2
CRIv2	Emissions	4.8	7.9	10.8
	Chemistry	6.0	11.1	13.7
MOZART-4	Emissions	4.1	6.7	10.0
	Chemistry	6.0	10.2	12.3
CB05	Emissions	4.6	7.4	9.8
	Chemistry	9.3	16.0	19.9
RADM2	Emissions	3.8	5.7	7.8
	Chemistry	8.6	14.1	17.3

isoprene emissions with temperature. The estimated emissions of isoprene with MEGAN2.1 using these assumptions are illustrated in Fig. 1 and show the expected exponential increase in isoprene emissions with temperature (Guenther et al., 2006).

The estimated emissions of isoprene at 20 °C lead to 0.07 ppbv of isoprene in our simulations while at 30 °C, the increased emissions of isoprene using MEGAN2.1 estimations lead to 0.35 ppbv of isoprene in the model. A measurement campaign over Essen, Germany (Wagner and Kuttler, 2014) measured 0.1 ppbv of isoprene at temperature 20 °C and 0.3 ppbv of isoprene were measured at 30 °C. The similarity of the simulated and observed isoprene mixing ratios indicates that the MEGAN2.1 variables chosen for calculating the temperature-dependent emissions of isoprene were suitable for simulating urban conditions over central Europe.

3   Results and Discussion

3.1   Ozone as a Function of NO_x and Temperature

Figure 2 depicts the maximum mixing ratio of ozone as a function of the total NO_x emissions on the first day of simulations and temperature when using a temperature-independent and temperature-dependent source of isoprene emissions for each chemical mechanism. A non-linear relationship of ozone mixing ratios with NO_x and temperature is reproduced by each chemical mechanism. This non-linear relationship is similar to that determined by Pusede et al. (2014) using an analytical model constrained to observational measurements over the San Joaquin Valley in California.

Higher ozone mixing ratios are produced when using a temperature-dependent source of

Figure 2: Contours of maximum ozone mixing ratios (ppbv) as a function of the total NO$_x$ emissions on the first day and temperature for each chemical mechanism using a temperature-dependent and temperature-independent source of isoprene emissions.
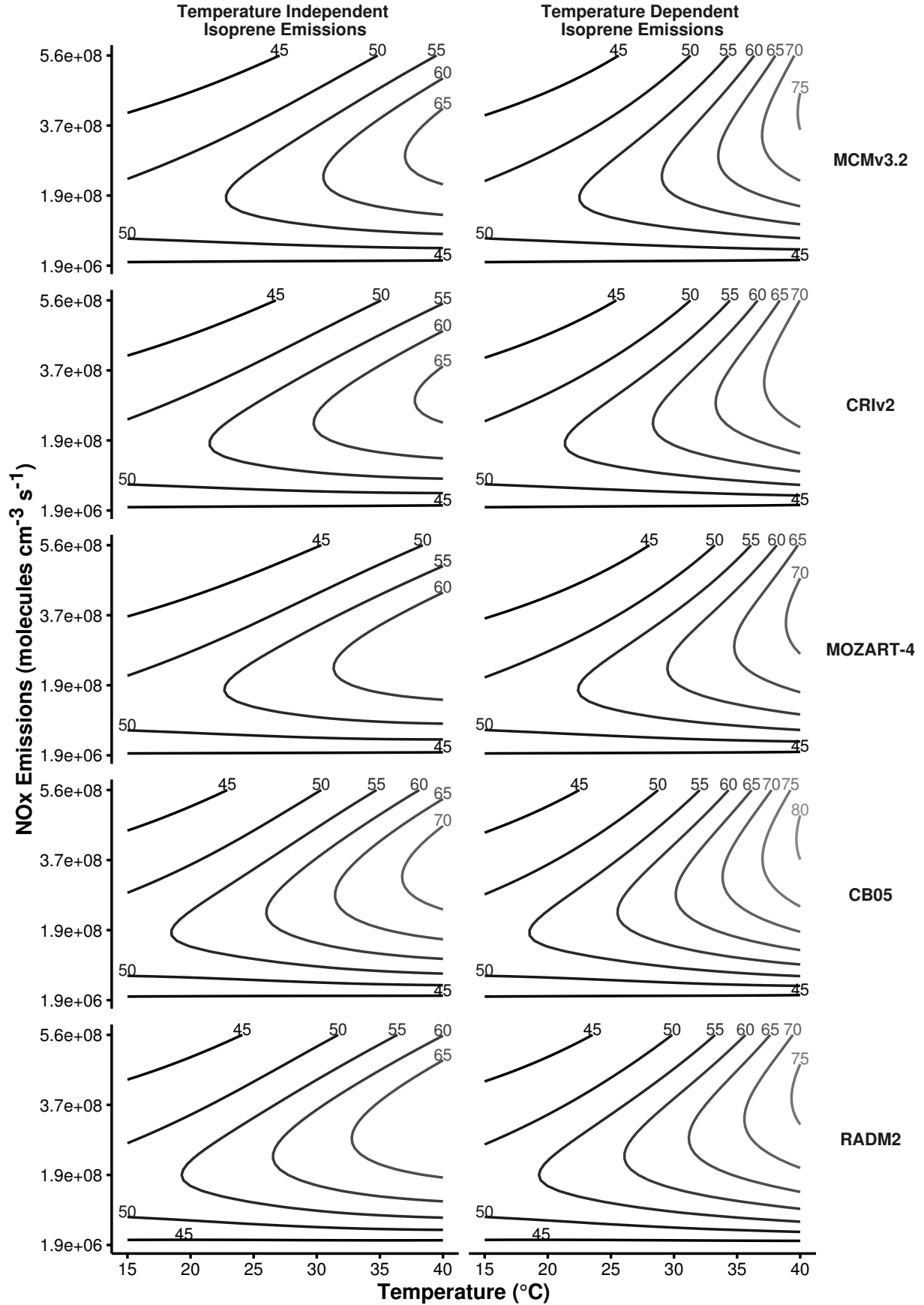
Figure 3: Ozone mixing ratios (ppbv) at each temperature are allocated to different NO_x-regimes of Fig. 2. The differences in ozone mixing ratios due to chemistry (solid line) and emissions (dotted line) are represented graphically for MOZART-4 with High-NO_x conditions and summarised in Table 2, the approach was used to calculate the differences with each chemical mechanism.
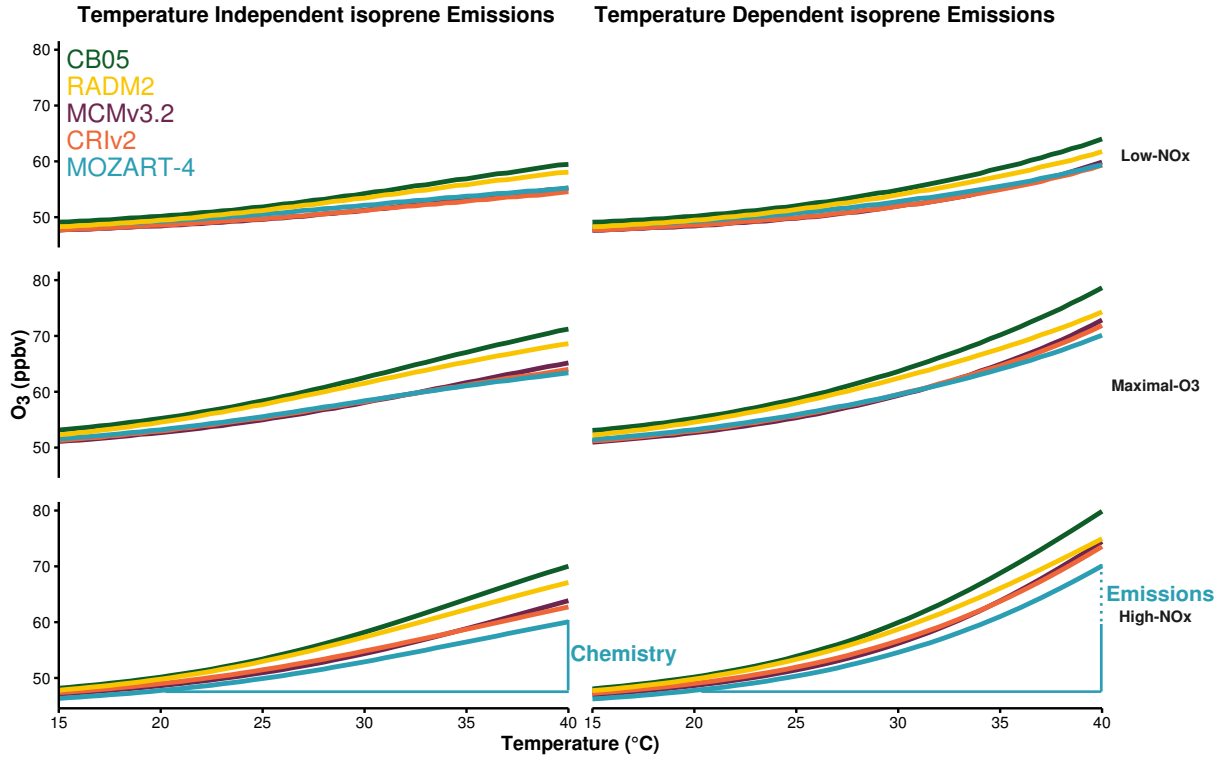
^{173} isoprene emissions (Fig. 2). The highest mixing ratios of ozone are produced at high temperatures

^{174} and moderate emissions of NO_x regardless of the source of isoprene emissions. Conversely, the

^{175} least amount of ozone is produced with low emissions of NO_x over the whole temperature range

^{176} (15 – 40 °C) when using both a temperature-independent and temperature-dependent source of

^{177} isoprene emissions.

^{178} The contours of ozone mixing ratios as a function of NO_x and temperature can be split into

^{179} three NO_x regimes (Low-NO_x, Maximal-O_3 and High-NO_x), similar to the NO_x regimes defined for

^{180} the non-linear relationship of ozone with VOC and NO_x. The Low-NO_x regime corresponds with

^{181} regions with little increase in ozone with temperature, also called the NO_x-sensitive regime. The

^{182} High-NO_x (or NO_x-saturated) regime is when ozone levels increase rapidly with temperature and

^{183} the contour ridges correspond to regions of maximal ozone production. This is the Maximal-O_3

^{184} regime. Pusede et al. (2014) showed that temperature can be used as a proxy for VOC, thus

^{185} we assigned the ozone mixing ratios from each box model simulation to a NO_x regime based on

^{186} the ratio of HNO_3 to H_2O_2. This ratio was used by Sillman (1995) to designate ozone to NO_x

^{187} regimes based on NO_x and VOC levels.

^{188} Fig. 3 illustrates the mean ozone mixing ratio at each temperature in the NO_x regimes for

each chemical mechanism and each type of isoprene emissions (temperature independent and temperature dependent). We define the absolute increase in ozone at 40 °C from 20 °C due to faster reaction rates as the difference between ozone mixing ratios at 40 °C and 20 °C when using a temperature-independent source of isoprene emissions. When using a temperature-dependent source of isoprene emissions, the difference in ozone mixing ratios at 40 °C from 20 °C minus the increase due to faster chemistry, gives the absolute increase in ozone due to increased isoprene emissions. These differences are represented graphically in Fig. 3 and summarised in Table 2.

Table 2 shows that the absolute increase in ozone with temperature due to faster chemistry is larger than the absolute increase in ozone due to increased isoprene emissions for each chemical mechanism and each NO_x regime. In all cases the absolute increase in ozone is largest under High-NO_x conditions and lowest with Low-NO_x conditions (Fig. 3 and Table 2). The increase in ozone mixing ratio at 40 °C from 20 °C due to faster chemistry with High-NO_x conditions is almost double that under Low-NO_x conditions.

In the Low-NO_x regime, the increase of ozone with temperature using the reduced chemical mechanisms (CRIv2, MOZART-4, CB05 and RADM2) is similar to that from the MCMv3.2, larger differences occur in the Maximal-O_3 and High-NO_x regimes. All reduced chemical mechanisms except RADM2 have similar increases in ozone due to increased isoprene emissions to MCMv3.2 (Table 2). RADM2 produces 3 ppbv less ozone than the MCMv3.2 due to increased isoprene emissions in each NO_x regime, indicating that this difference is due the representation of isoprene degradation chemistry in RADM2. These differences between the chemical mechanisms shall be explored in Sect. 3.2.

The Tagged Ozone Production Potential (TOPP) defined in Butler et al. (2011) is a measure of the number of molecules of ozone produced per molecule of VOC emitted. Coates and Butler (2015) compared ozone production in different chemical mechanisms to the MCMv3.2 using TOPPs and showed that less ozone is produced per molecule of isoprene emitted using RADM2 than with MCMv3.2. The degradation of isoprene has been extensively studied and it is well-known that methyl vinyl ketone (MVK) and methacrolein are signatures of isoprene degradation (Atkinson, 2000). All chemical mechanisms in our study except RADM2 explicitly represent MVK and methacrolein (or in the case of CB05, a lumped species representing both these secondary degradation products). RADM2 does not represent methacrolein and the mechanism species representing ketones (KET) is a mixture of acetone and methyl ethyl ketone (MEK) (Stockwell et al., 1990). Thus the secondary degradation of isoprene in RADM2 is

Figure 4: Day-time budgets of O_x normalised by the total oxidation rate of emitted VOC in the NO_x-regimes of Fig. 3. The white line indicates net production or consumption of O_x. The net contribution of reactions to O_x budgets are allocated to categories of deposition, inorganic reactions, peroxy nitrates (RO2NO2), reactions of NO with HO2, alkyl peroxy radicals (RO2) and acyl peroxy radicals (ARO2). All other reactions contributing to O_x budgets are allocated to the 'Other Organic' category.
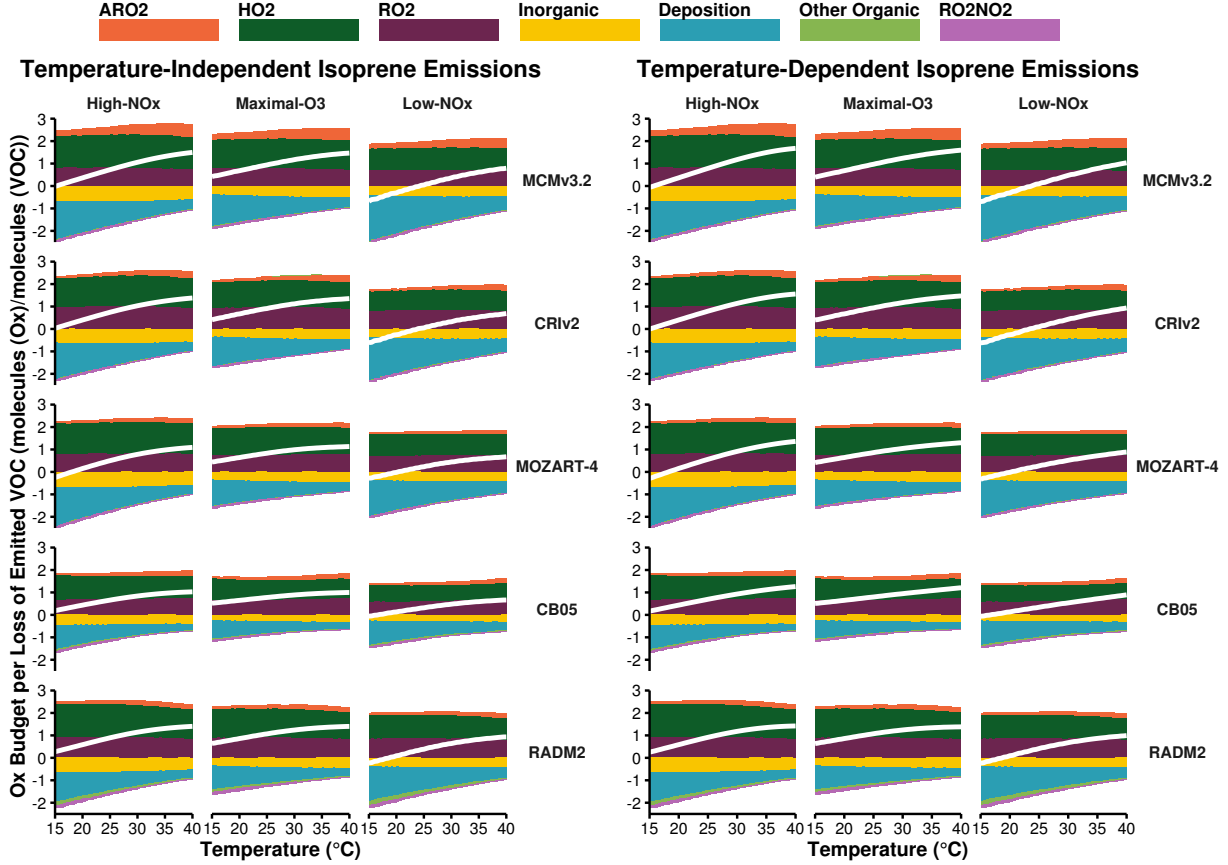
unable to represent the ozone production from the further degradation of the signature secondary degradation products of isoprene, MVK and methacrolein. Updated versions of RADM2, RACM (Stockwell et al., 1997) and RACM2 (Goliff et al., 2013), sequentially included methacrolein and MVK and with these updates the TOPP value of isoprene approached that of the MCMv3.2 (Coates and Butler, 2015).

3.2 Ozone Production Budgets

The day-time production and consumption budgets of O_x $(\equiv O_3 + NO_2 + O + O(^1D))$ normalised by the total rate of oxidation of the emitted VOC are displayed in Fig. 4. The O_x budgets are assigned to each NO_x regime for each chemical mechanism and type of isoprene emissions. The budgets are allocated to the net contribution of major sources, where 'HO2', 'RO2', 'ARO2' represent the reactions of NO with HO_2, alkyl peroxy radicals and acyl peroxy radicals respectively. 'RO2NO2' represents the effects of peroxy nitrates, 'Deposition' represents ozone deposition,

'Inorganic' is all other inorganic contributions to O_x production and any other remaining organic reactions are included in the 'Other Organic' category. Figure 4 also illustrates the net production or consumption of O_x in each case.

The net O_x production efficiency increases from 20 °C to 40 °C by $\sim$ 1 molecule of O_x per molecule of VOC oxidised using both temperature-dependent and temperature-independent isoprene emissions and in each NO_x condition (Fig. 4). The increase in net O_x production efficiency is due to a decrease in the consumption efficiency of O_x with temperature while the production efficiency of O_x remains constant with temperature ($\sim$ 2 molecules of O_x per molecule of VOC). The decrease in ozone deposition per VOC loss from 20 °C to 40 °C of $\sim$ 1 molecule of O_x per loss of VOC mirrors the increase in net O_x production efficiency.

As the production efficiency of O_x remains constant with temperature in Fig. 4, the rate of O_x production is controlled by the loss rate of the VOCs. Faster oxidation of VOCs leads to a faster production rate with temperature of peroxy radicals which when converting NO to NO_2 produce more ozone with temperature. The review of Pusede et al. (2015) also acknowledged the importance of organic reactivity and radical production to the ozone-temperature relationship. Also, the modelling study of Steiner et al. (2006) noted that the increase in initial oxidation rates of VOCs with temperature leads to increased formaldehyde concentrations and since formaldehyde is an important source of radicals leading to an increase of ozone with temperature.

The net effect of peroxy nitrates on O_x production efficiency in our study is negligible, contributing to a decrease in $\sim$ 0.1 molecules of O_x per VOC oxidised at 40 °C from 20 °C. Peroxynitrates are produced from the reactions of acyl peroxy radicals with NO_2 and are an important reservoir of both peroxy radicals and NO_x. The decomposition rate of peroxy nitrates is strongly temperature dependent, thus at higher temperatures the faster decomposition rate leads to faster re-release of peroxy radicals and NO_x influencing the production of ozone. This lack of influence of RO2NO2 on the net production efficiency of O_x is rather surprising given that many other studies cite the decrease in the lifetime of peroxy nitrates as one of the most important factors for the increase of ozone with temperature. For example, Dawson et al. (2007) attributed the increase in ozone with temperature during a modelling study over the eastern US to the decrease in PAN lifetime with temperature. Steiner et al. (2006) also recognised that the decrease in PAN lifetime with temperature may contribute to the increase of ozone with temperature and concluded that the combined effects of increased VOC reactivity and PAN decomposition are most likely to increase the production of ozone with tempeature.

The increase in ozone with temperature also leads to an increase in OH with temperature through the following reaction sequence.

$$O_3 + h\nu \rightarrow O(^1D) + O_2 \tag{R1}$$

$$O(^1D) + H_2O \rightarrow OH + OH \tag{R2}$$

The degradation of VOCs after reaction with OH results in either net production or consumption of ozone depending on the NO_x conditions. In low-NO_x conditions, peroxy radicals produced from the degradation of VOCs are more likely to react with other peroxy radicals leading to a net sink of ozone. With increasing NO_x levels, peroxy radicals may react with NO producing NO_2 leading to net ozone production depending on the number of peroxy radicals produced during VOC degradation. Increasing NO_x levels even further increases nitric acid formation from the reaction of OH and NO_2 limiting ozone production. This non-linear chemistry of ozone production is evident in Fig. 2.

The degradation of VOCs recycles OH during the reactions of many secondary degradation products. For example, OH and NO_2 are the products of the reaction of HO_2 with NO which has the largest single contribution to the O_x production efficiency (Fig. 4). Thus showing the strong coupling of the increase of ozone and OH with temperature.

3.3 Comparison to Observations and 3D Model Simulations

This section compares the results from our idealised box model simulations to real-world observations and model output from a 3D model. Otero et al. (2016) showed that over the summer (JJA) months, temperature is the main meteorological driver of ozone production over many regions of central Europe using the observational data set of the ERA-Interim re-analysis. This data set includes the daily maximum temperature and daily maximum 8 h mean of ozone for the years 1998–2012 over Europe. Model output from the 3D WRF-Chem regional model set-up over the European domain for simulations of the year 2007 using MOZART-4 chemistry from Mar et al. (2016) was used to further compare the box model simulations to a model including more meteorological processes than the box model.

Figure 5 compares the observational (ERA-Interim) and WRF-Chem data from summer 2007 to the maximum 8 h mean ozone from the box model simulations for each chemical mechanism, NO_x regime and type of isoprene emissions. In Fig. 5, we limited the observational data to days

13

Figure 5: The maximum 8 h mean ozone from the box model simulations allocated to the different NO_x regimes for each chemical mechanisms (solid lines). The box model ozone-temperature correlation is compared to the summer 2007 ERA-Interim data (black circles) and WRF-Chem output (purple boxes).
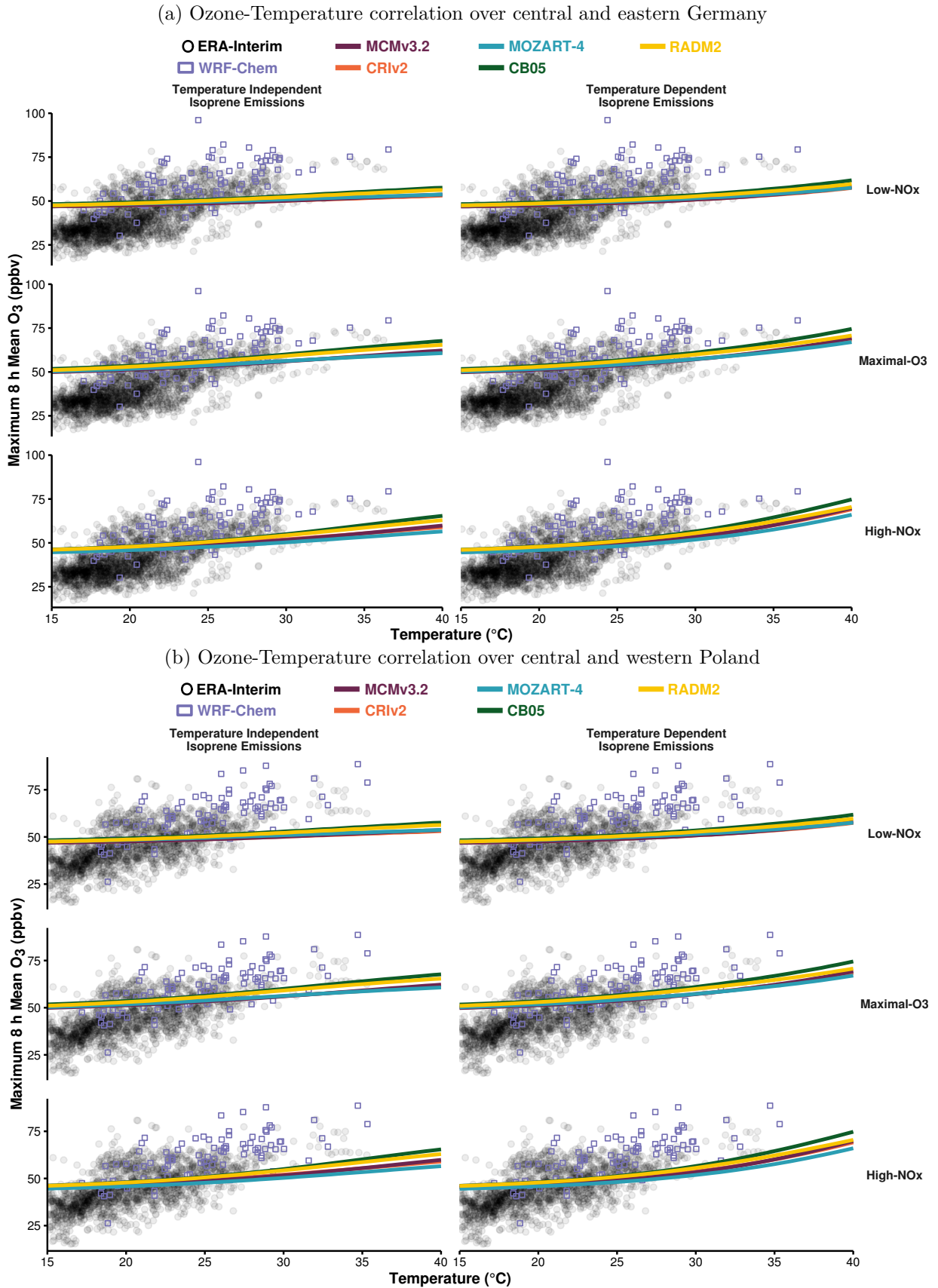
(a) Ozone-Temperature correlation over central and eastern Germany

(b) Ozone-Temperature correlation over central and western Poland

Table 3: Slopes (m_{O3-T} in ppbv per °C) of the linear fit to the ozone-temperature correlations in Fig. 5

(a) Slope of linear fit of the ERA-Interim observational data and WRF-Chem model output chemistry over central and eastern Germany and western and central Poland.

	Germany	Poland
ERA-Interim	2.15	1.94
WRF-Chem with MOZART-4	2.05	2.00

(b) Slope of linear fit of box model experiments for each chemical mechanism, source of isoprene emissions allocated to the three NO_x-regimes.

Mechanism	Isoprene Emissions	Low-NO_x	Maximal-O_3	High-NO_x
MCMv3.2	Temperature Independent	0.28	0.51	0.59
	Temperature Dependent	0.42	0.74	0.93
CRIv2	Temperature Independent	0.25	0.47	0.55
	Temperature Dependent	0.40	0.71	0.90
MOZART-4	Temperature Independent	0.25	0.44	0.49
	Temperature Dependent	0.38	0.65	0.81
CB05	Temperature Independent	0.39	0.67	0.79
	Temperature Dependent	0.52	0.89	1.12
RADM2	Temperature Independent	0.37	0.61	0.70
	Temperature Dependent	0.48	0.79	0.97

where the observed daily maximum temperature corresponded to the temperature range in our study (15–40 °C). We selected two regions from the observations and WRF-Chem output, central and eastern Germany (Fig. 5a) and central and western Poland (Fig. 5b), where the summertime ozone values are driven by with temperature (Otero et al., 2016). Table 3 summarises the slopes (m_{O3-T}) of the linear fits of all the ozone-temperature correlations displayed in Fig. 5 in ppbv of ozone per °C determining the rate of change of ozone with temperature.

The spread of the observed ozone-temperature values over both Germany and Poland are generally captured by the combined WRF-Chem simulations. However, the ozone-temperature data from WRF-Chem reproduces the higher ozone values with temperature from ERA-Interim but not the lower values. The rate of change of ozone with temperature from the WRF-Chem simulations is similar to the rate of change of ozone with temperature from the observed data (Table 3a).

The differences in ozone production between the different chemical mechanisms with the box model are small compared to the spread of the ERA-Interim and WRF-Chem data. When using a temperature-dependent source of isoprene emissions in the box model, the rate of change of

ozone with temperature in the box model approaches that of the observed data, although still less than half that of the observations. The box model simulations using a temperature-independent source of isoprene emissions do not reproduce the range of observed ozone-temperature values (Table 3).

A temperature-dependent source of isoprene with high-NO_x conditions produces the most similar ozone-temperature slope to the observational data but this is still lower than the observed ozone-temperature slope by a factor of two. In particular, the box model simulations over-predict the ozone values at lower temperatures and under-predict the ozone values at higher temperatures compared to the observed data. Similarly, the rate of change of ozone with temperature in the box model is less-sensitive than WRF-Chem.

The main reason for the box model simulations being less sensitive to temperature than the observations and WRF-Chem simulations is related to the set-up of the box model. In our simulations, we focused on instantaneous production of ozone from a freshly-emitted source of VOC not considering stagnant atmospheric conditions which are characterised by high temperatures and low wind speeds slowing the transport of ozone and its precursors away from sources. Otero et al. (2016) showed that the previous day's ozone was also an important driver for observed ozone production over Europe also Jacob et al. (1993) correlated high-ozone episodes in the summer over eastern US to regional stagnation.

Stagnantion is an example of the coupling of meteorological variables, in this case temperature and wind speed, impacting ozone production. In observational studies, which look at the total derivative of ozone with temperature, the direct effects of temperature (e.g. increasing reaction rates, emissions from vegetation) and indirect (e.g. heatwaves characterised by high temperatures and low wind speed) effects of temperature on ozone are not easily separated. In other words, observational studies represent the total derivative of ozone with temperature while models consider the partial derivatives of the temperature-dependent processes influencing ozone (Rasmussen et al., 2013).

$$\frac{d[\text{O}_3]}{dT} = \frac{\partial[\text{O}_3]}{\partial[\text{BVOC}]}\frac{\partial[\text{BVOC}]}{\partial T} + \frac{\partial[\text{O}_3]}{\partial\text{Chemistry}}\frac{\partial\text{Chemistry}}{\partial T} + \frac{\partial[\text{O}_3]}{\partial\text{Stagnation}}\frac{\partial\text{Stagnation}}{\partial T} + \dots$$

3D models such as WRF-Chem that can simulate more realistic atmospheric conditions would play a valuable role for future work evaluating the ozone-temperature relationship at different NO_x conditions at a regional scale.

4 Conclusions

In this study, we determined the effects of temperature on ozone production using a box model over a range of temperatures and NO_x conditions with a temperature-independent and temperature-dependent source of isoprene emissions. These simulations were repeated using reduced chemical mechanism schemes (CRIv2, MOZART-4, CB05 and RADM2) typically used in 3D models and compared to the near-explicit MCMv3.2 chemical mechanism.

Each chemical mechanism produced a non-linear relationship of ozone with temperature and NO_x with the most ozone produced at high temperatures and high emissions of NO_x. Conversely, lower NO_x levels led to a minimal increase of ozone with at all temperatures. Thus air quality in a future with higher temperatures predicted with climate change would benefit from dramatical reductions in NO_x emissions.

Faster chemistry at higher temperatures was responsible for a greater absolute increase in ozone than increased isoprene emissions. Faster thermal decomposition of peroxy nitrates at higher temperatures contributed the most to ozone production with each chemical mechanism and all NO_x conditions. The contribution of peroxy nitrates using reduced chemical mechanisms (CRIv2, MOZART-4, CB05, RADM2) was less than the reference MCMv3.2 chemical mechanisms. The differences were mainly due to the inclusion of methylperoxy nitrate ($CH_3O_2NO_2$) chemistry in MCMv3.2 that is not included in any of the reduced chemical mechanisms used in this study. Including methylperoxy nitrate chemistry in reduced chemical mechanisms would minimise the differences in the production of ozone from reduced chemical mechanisms to the MCMv3.2 at higher temperatures.

The rate of change of ozone with temperature using observational data (ERA-Interim) over Europe was twice as high as when using the box model. This was due to the box model not representing stagnant atmospheric conditions that are inherently included in observational data and models including meteorology, such as WRF-Chem. Future work looking at the influence of temperature on ozone should include stagnant conditions to represent more realistic atmospheric conditions. Any modelling work addressing this should also consider a range of NO_x conditions as this strongly influenced the amount of ozone produced in our study.

References

Roger Atkinson. Atmospheric chemistry of VOCs and NO_x. *Atmospheric Environment*, 34(12-14): 2063–2101, 2000.

A. Baklanov, K. Schlünzen, P. Suppan, J. Baldasano, D. Brunner, S. Aksoyoglu, G. Carmichael, J. Douros, J. Flemming, R. Forkel, S. Galmarini, M. Gauss, G. Grell, M. Hirtl, S. Joffre, O. Jorba, E. Kaas, M. Kaasik, G. Kallos, X. Kong, U. Korsholm, A. Kurganskiy, J. Kushta, U. Lohmann, A. Mahura, A. Manders-Groot, A. Maurizi, N. Moussiopoulos, S. T. Rao, N. Savage, C. Seigneur, R. S. Sokhi, E. Solazzo, S. Solomos, B. Sørensen, G. Tsegas, E. Vignati, B. Vogel, and Y. Zhang. Online coupled regional meteorology chemistry models in Europe: current status and prospects. *Atmospheric Chemistry and Physics*, 14(1):317–398, 2014.

T.M. Butler, M.G. Lawrence, D. Taraborrelli, and J. Lelieveld. Multi-day ozone production potential of volatile organic compounds calculated with a tagging approach. *Atmospheric Environment*, 45(24):4082 – 4090, 2011.

William P. L. Carter. Development of a Database for Chemical Mechanism Assignments for Volatile Organic Emissions. *Journal of the Air & Waste Management Association*, 0, 2015.

William P. L. Carter, Arthur M. Winer, Karen R. Darnall, and James N. Pitts Jr. Smog chamber studies of temperature effects in photochemical smog. *Environmental Science & Technology*, 13 (9):1094–1100, 1979.

J. Coates and T. M. Butler. A comparison of chemical mechanisms using tagged ozone production potential (TOPP) analysis. *Atmospheric Chemistry and Physics*, 15(15):8795–8808, 2015.

John P. Dawson, Peter J. Adams, and Spyros N. Pandis. Sensitivity of ozone to summertime climate in the eastern USA: A modeling case study . *Atmospheric Environment*, 41(7):1494 – 1511, 2007.

K. M. Emmerson and M. J. Evans. Comparison of tropospheric gas-phase chemistry schemes for use within global models. *Atmospheric Chemistry and Physics*, 9(5):1831–1845, 2009.

L. K. Emmons, S. Walters, P. G. Hess, J.-F. Lamarque, G. G. Pfister, D. Fillmore, C. Granier, A. Guenther, D. Kinnison, T. Laepple, J. Orlando, X. Tie, G. Tyndall, C. Wiedinmyer, S. L. Baughcum, and S. Kloster. Description and evaluation of the Model for Ozone and Related chemical Tracers, version 4 (MOZART-4). *Geoscientific Model Development*, 3(1):43–67, 2010.

Wendy S. Goliff, William R. Stockwell, and Charlene V. Lawson. The regional atmospheric chemistry mechanism, version 2. *Atmospheric Environment*, 68:174 – 185, 2013.

A. Guenther, T. Karl, P. Harley, C. Wiedinmyer, P. I. Palmer, and C. Geron. Estimates of global terrestrial isoprene emissions using MEGAN (Model of Emissions of Gases and Aerosols from Nature). *Atmospheric Chemistry and Physics*, 6(11):3181–3210, 2006.

A. B. Guenther, X. Jiang, C. L. Heald, T. Sakulyanontvittaya, T. Duhl, L. K. Emmons, and X. Wang. The Model of Emissions of Gases and Aerosols from Nature version 2.1 (MEGAN2.1): an extended and updated framework for modeling biogenic emissions. *Geoscientific Model Development*, 5(6):1471–1492, 2012.

Shiro Hatakeyama, Hajime Akimoto, and Nobuaki Washida. Effect of temperature on the formation of photochemical ozone in a propene-nitrogen oxide (NOx)-air-irradiation system. *Environmental Science & Technology*, 25(11):1884–1890, 1991.

Daniel J. Jacob and Darrell A. Winner. Effect of climate change on air quality. *Atmospheric Environment*, 43(1):51 – 63, 2009. Atmospheric Environment - Fifty Years of Endeavour.

Daniel J Jacob, Jennifer A Logan, Geraldine M Gardner, Rose M Yevich, Clarisa M Spivakovsky, Steven C Wofsy, Sanford Sillman, and Michael J Prather. Factors regulating ozone over the united states and its export to the global atmosphere. *Journal of Geophysical Research*, 98(D8), 1993.

M. E. Jenkin, S. M. Saunders, V. Wagner, and M. J. Pilling. Protocol for the development of the Master Chemical Mechanism, MCM v3 (Part B): tropospheric degradation of aromatic volatile organic compounds. *Atmospheric Chemistry and Physics*, 3(1):181–193, 2003.

M.E. Jenkin, L.A. Watson, S.R. Utembe, and D.E. Shallcross. A Common Representative Intermediates (CRI) mechanism for VOC degradation. Part 1: Gas phase mechanism development. *Atmospheric Environment*, 42(31):7185 – 7195, 2008.

Michael E. Jenkin, Sandra M. Saunders, and Michael J. Pilling. The tropospheric degradation of volatile organic compounds: a protocol for mechanism development. *Atmospheric Environment*, 31(1):81 – 104, 1997.

J. J. P. Kuenen, A. J. H. Visschedijk, M. Jozwicka, and H. A. C. Denier van der Gon. TNO-MACC_II emission inventory; a multi-year (2003–2009) consistent high-resolution european

emission inventory for air quality modelling. *Atmospheric Chemistry and Physics*, 14(20): 10963–10976, 2014.

K. A. Mar, N. Ojha, A. Pozzer, and T. M. Butler. WRF-Chem Simulations over Europe: Model Evaluation and Chemical Mechanism Comparison. *In Preparation*, 2016.

N. Otero, J. Sillmann, J. L. Schnell, H. W. Rust, and T. Butler. Synoptic and meteorological drivers of extreme ozone concentrations over europe. *Environmental Research Letters*, 11(2): 024005, 2016.

N. Passant. Speciation of UK emissions of non-methane volatile organic compounds. Technical report, DEFRA, Oxon, UK., 2002.

George Pouliot, Hugo A.C. Denier van der Gon, Jeroen Kuenen, Junhua Zhang, Michael D. Moran, and Paul A. Makar. Analysis of the emission inventories and model-ready emission datasets of Europe and North America for phase 2 of the AQMEII project. *Atmospheric Environment*, 115: 345–360, 2015.

S. E. Pusede, D. R. Gentner, P. J. Wooldridge, E. C. Browne, A. W. Rollins, K.-E. Min, A. R. Russell, J. Thomas, L. Zhang, W. H. Brune, S. B. Henry, J. P. DiGangi, F. N. Keutsch, S. A. Harrold, J. A. Thornton, M. R. Beaver, J. M. St. Clair, P. O. Wennberg, J. Sanders, X. Ren, T. C. VandenBoer, M. Z. Markovic, A. Guha, R. Weber, A. H. Goldstein, and R. C. Cohen. On the temperature dependence of organic reactivity, nitrogen oxides, ozone production, and the impact of emission controls in San Joaquin Valley, California. *Atmospheric Chemistry and Physics*, 14(7):3373–3395, 2014.

Sally E. Pusede, Allison L. Steiner, and Ronald C. Cohen. Temperature and Recent Trends in the Chemistry of Continental Surface Ozone. *Chemical Reviews*, 115(10):3898–3918, 2015.

D. J. Rasmussen, Jianlin Hu, Abdullah Mahmud, and Michael J. Kleeman. The ozone–climate penalty: Past, present, and future. *Environmental Science & Technology*, 47(24):14258–14266, 2013. PMID: 24187951.

Andrew Rickard, Jenny Young, M. J. Pilling, M. E. Jenkin, Stephen Pascoe, and S. M. Saunders. The Master Chemical Mechanism Version MCM v3.2. `http://mcm.leeds.ac.uk/MCMv3.2/`, 2015. [Online; accessed 25-March-2015].

Juli I. Rubin, Andrew J. Kean, Robert A. Harley, Dylan B. Millet, and Allen H. Goldstein. Temperature dependence of volatile organic compound evaporative emissions from motor vehicles. *Journal of Geophysical Research: Atmospheres*, 111(D3), 2006. D03305.

S. M. Saunders, M. E. Jenkin, R. G. Derwent, and M. J. Pilling. Protocol for the development of the Master Chemical Mechanism, MCM v3 (Part A): tropospheric degradation of non-aromatic volatile organic compounds. *Atmospheric Chemistry and Physics*, 3(1):161–180, 2003.

Sanford Sillman. The use of NOy, H2O2, and HNO3 as indicators for ozone-NOx-hydrocarbon sensitivity in urban locations. *Journal of Geophysical Research: Atmospheres*, 100(D7): 14175–14188, 1995.

Sanford Sillman. The relation between ozone, NOx and hydrocarbons in urban and polluted rural environments. *Atmospheric Environment*, 33(12):1821 – 1845, 1999.

Sanford Sillman and Perry J. Samson. Impact of temperature on oxidant photochemistry in urban, polluted rural and remote environments. *Journal of Geophysical Research: Atmospheres*, 100(D6):11497–11508, 1995.

D. Simpson, A. Benedictow, H. Berge, R. Bergström, L. D. Emberson, H. Fagerli, C. R. Flechard, G. D. Hayman, M. Gauss, J. E. Jonson, M. E. Jenkin, A. Nyíri, C. Richter, V. S. Semeena, S. Tsyro, J.-P. Tuovinen, Á. Valdebenito, and P. Wind. The EMEP MSC-W chemical transport model – technical description. *Atmospheric Chemistry and Physics*, 12(16):7825–7865, 2012.

Allison L. Steiner, Shaheen Tonse, Ronald C. Cohen, Allen H. Goldstein, and Robert A. Harley. Influence of future climate and emissions on regional air quality in California. *Journal of Geophysical Research: Atmospheres*, 111(D18), 2006. D18303.

William R. Stockwell, Paulette Middleton, Julius S. Chang, and Xiaoyan Tang. The second generation regional acid deposition model chemical mechanism for regional air quality modeling. *Journal of Geophysical Research: Atmospheres*, 95(D10):16343–16367, 1990.

William R. Stockwell, Frank Kirchner, Michael Kuhn, and Stephan Seefeld. A new mechanism for regional atmospheric chemistry modeling. *Journal of Geophysical Research: Atmospheres*, 102(D22):25847–25879, 1997.

E. von Schneidemesser, J. Coates, A. J. H. Visschedijk, H. A. C. Denier van der Gon, and T. M.

Butler. Variation of the NMVOC speciation in the solvent sector and the sensitivity of modelled tropospheric ozone. *Atmospheric Environment*, Submitted for Publication, 2016.

Erika von Schneidemesser, Paul S. Monks, James D. Allan, Lori Bruhwiler, Piers Forster, David Fowler, Axel Lauer, William T. Morgan, Pauli Paasonen, Mattia Righi, Katerina Sindelarova, and Mark A. Sutton. Chemistry and the Linkages between Air Quality and Climate Change. *Chemical Reviews*, 2015. PMID: 25926133.

Patrick Wagner and Wilhelm Kuttler. Biogenic and anthropogenic isoprene in the near-surface urban atmosphere — A case study in Essen, Germany. *Science of The Total Environment*, 475: 104 – 115, 2014.

Greg Yarwood, Sunja Rao, Mark Yocke, and Gary Z. Whitten. Updates to the Carbon Bond Chemical Mechanism: CB05. Technical report, U. S Environmental Protection Agency, 2005.